Available online at www.sciencedirect.com
ScienceDirect
Geochimica et Cosmochimica Acta 74 (2010) 928–940
Geochimica et Cosmochimica Acta
www.elsevier.com/locate/gca

The impact of salinity on the Mg/Ca and Sr/Ca ratio in the benthic foraminifera *Ammonia tepida*: Results from culture experiments

Delphine Dissard [a,*], Gernot Nehrke [a], Gert Jan Reichart [a,b], Jelle Bijma [a]

[a] *Alfred Wegener Institute for Polar and Marine Research, Bremerhaven, Germany*
[b] *Faculty of Geosciences, Utrecht University, The Netherlands*

Received 6 February 2009; accepted in revised form 23 October 2009; available online 31 October 2009

Abstract

Over the last decade, sea surface temperature (SST) reconstructed from the Mg/Ca ratio of foraminiferal calcite has increasingly been used, in combination with the $\delta^{18}O$ signal measured on the same material, to calculate the $\delta^{18}O_w$, a proxy for sea surface salinity (SSS). A number of studies, however, have shown that the Mg/Ca ratio is also sensitive to other parameters, such as pH or $[CO_3^{2-}]$, and salinity. To increase the reliability of foraminiferal Mg/Ca ratios as temperature proxies, these effects should be quantified in isolation. Individuals of the benthic foraminifera *Ammonia tepida* were cultured at three different salinities (20, 33 and 40 psu) and two temperatures (10–15 °C). The Mg/Ca and Sr/Ca ratios of newly formed calcite were analyzed by Laser Ablation ICP-MS and demonstrate that the Mg concentration in *A. tepida* is overall relatively low (mean value per experimental condition between 0.5 and 1.3 mmol/mol) when compared to other foraminiferal species, Sr being similar to other foraminiferal species. The Mg and Sr incorporation are both enhanced with increasing temperatures. However, the temperature dependency for Sr disappears when the distribution factor D_{Sr} is plotted as a function of calcite saturation state (Ω). This suggests that a kinetic process related to Ω is responsible for the observed dependency of Sr incorporation on sea water temperature. The inferred relative increase in D_{Mg} per unit salinity is 2.8% at 10 °C and 3.3% at 15 °C, for the salinity interval 20–40 psu. This implies that a salinity increase of 2 psu results in enhanced Mg incorporation equivalent to 1 °C temperature increase. The D_{Sr} increase per unit salinity is 0.8% at 10 °C and 1.3% at 15 °C, for the salinity interval 20–40 psu.

1. INTRODUCTION

To understand past changes in ocean circulation, records of both temperature and salinity are required to reconstruct density fields. The Mg/Ca ratio in foraminiferal calcite, combined with its oxygen isotopic composition, became one of the most widely applied proxies to deconvolve salinity and temperature. On timescales shorter than its residence time in the ocean, magnesium occurs in seawater with nearly constant ratios to calcium (Broecker and Peng, 1982). Variation in Mg/Ca in benthic foraminiferal tests can then be explained as a function of environmental parameters that control its incorporation into the tests. For foraminifera, temperature appears to be the dominant parameter (Nurnberg et al., 1996; Rathburn and DeDeckker, 1997; Rosenthal et al., 1997; Hastings et al., 1998; Lea et al., 1999; Toyofuku et al., 2000; Lear et al., 2002; Anand et al., 2003; Russell et al., 2004; Barker et al., 2005). However, a better understanding of vital effects and the impact of other parameters such as pH or $[CO_3^{2-}]$, and salinity is needed to increase the accuracy of element ratio proxies. Vital effects include: (1) physiological regulations, that are most probably genetically controlled and species dependent. (2) Ontogeny, possibly via growth rates, seems to drive

* Corresponding author. Tel.: +49 17667628088.
E-mail address: Delphine.Dissard@awi.de (D. Dissard).

0016-7037/$ - see front matter © 2009 Elsevier Ltd. All rights reserved.
doi:10.1016/j.gca.2009.10.040

intra-specimen variation (Elderfield et al., 2002; Anand and Elderfield, 2005; Hintz et al., 2006; Sadekov et al., 2008). (3) Symbiosis in some species adds another level of complexity as relative changes in symbiont activity with increasing test size may affect the elemental incorporation (Rink et al., 1998; Honisch and Hemming, 2004). Changes in $[CO_3^{2-}]$ seem to impact both Mg (Lea et al., 1999; Russell et al., 2004) and Sr (Rosenthal et al., 2006; Rathmann and Kuhnert, 2008) incorporation and an empirical relationship for the impact of $\Delta[CO_3^{2-}]$ on Mg/Ca was established for *Cibicidoides wuellerstorfi* (Elderfield et al., 2006).

The impact of salinity on Mg incorporation into foraminiferal calcite is poorly understood. Although it has been shown that salinity may affect the incorporation of Mg (Nurnberg et al., 1996; Lea et al., 1999; Ferguson et al., 2008; Kisakurek et al., 2008; Groeneveld et al., 2008), the lack of well constrained studies often led people to neglect it. Culture studies under constant physico-chemical conditions provide the best possible approach to isolate species-specific vital effects. In this study, we present results on Mg/Ca and Sr/Ca ratios from cultured specimens of the non-symbiotic shallow-water benthic species *Ammonia tepida*. Individuals were maintained under constant conditions at three different salinities (20, 33 and 40 psu) and two different temperatures (10 and 15 °C). Newly formed calcite (only of the final chamber) was analyzed for Mg and Sr by Laser Ablation-Inductively Coupled Plasma Mass Spectrometry (LA-ICP-MS).

2. MATERIAL AND METHODS

2.1. Collecting and culturing foraminifera

In spring 2006, live specimens of the symbiont-barren species *A. tepida* were collected at an intertidal flat of the Wadden Sea (near Dorum, Northwestern Germany). After transportation to the laboratory, the sediment containing foraminifera was sieved over a 630 μm mesh to remove the largest meiofauna, and kept in stock cultures. Less than 2 weeks after collection, living individuals of *Ammonia* (referred to as molecular type T6E by Hayward et al., 2004, further referred to as *A. tepida*) were picked from the stock cultures. They were screened under an inverted microscope (Zeiss Axiovert 200M) for pseudopodial activity (a sign for vitality) and living specimens were transferred to culture vessels. These culture vessels consisted of semi-closed aquaria containing filtered seawater (0.2 μm) kept at three different salinities. Salinities of 20, 33 and 40 psu were obtained either by dilution with deionised water, or evaporation at 50 °C, of natural seawater from the North Sea collected near Helgoland. Evaporation did not lead to any precipitates (e.g. calcium carbonate). To investigate the impact of varying Ca concentration (and hence saturation state, Ω) on the Mg and Sr incorporation, a second growth medium of salinity 20 psu was prepared and subsequently enriched by addition of $CaCl_2{\cdot}2H_2O$ (returning the Ca concentration to that of natural seawater with a salinity of 33 psu). This addition had no significant effect on salinity as the added $[Cl^-]$ is an order of magnitude lower than natural $[Cl^-]$. This medium is referred to as "salinity 20 + Ca". Samples of this Ca enriched medium were taken at the beginning and at the end of the experiment and measured via Inductively Coupled Plasma Optical Emission Spectrometry (ICP-OES). The constant Ca concentration during the incubations confirms that no inorganic calcite precipitated and that formation of new chambers by the foraminifera did not impact sea water concentrations. Foraminifera were fed at the beginning of the experiment and subsequently every 2 weeks with a mixture of dried algae (*Phaeodactylum tricornutum*, *Dunaliella salina*, and *Isochrisis galbana*). The fluorescent calcite stain calcein was added to each culture medium at a concentration of 5 mg/l. Incorporated calcein can be used to distinguish newly grown calcite (fluorescent) from pre-existing calcite (non-fluorescent) after termination of the experiments (Bernhard et al., 2004; Dissard et al., 2009) (Fig. 1). Only final chambers labelled with calcein were measured by LA-ICP-MS for their elemental composition. Culture experiments were conducted in two parallel series at 10 and 15 °C. In order

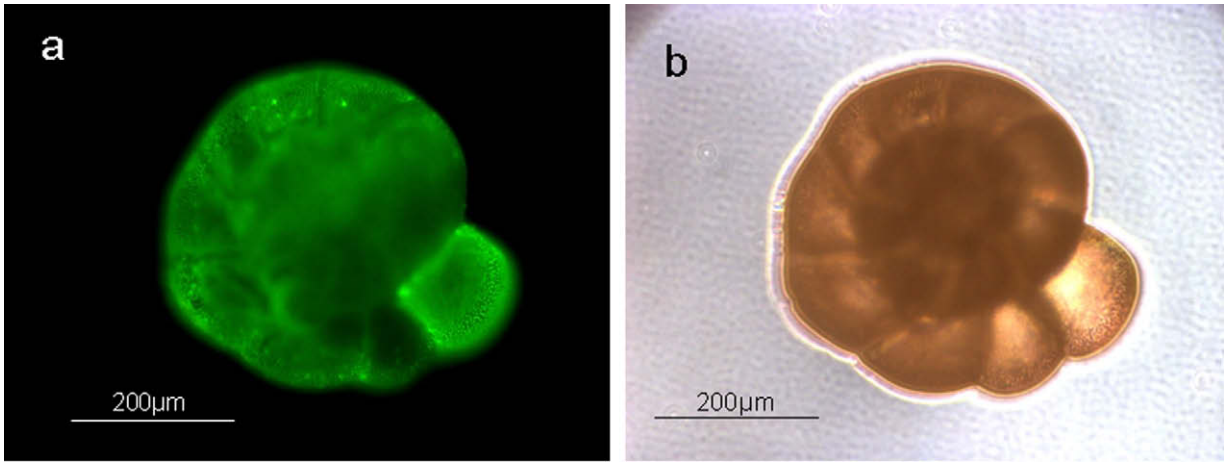

Fig. 1. (a) New chamber added by *Ammonia tepida* made visible by fluorescence of incorporated calcein. (b) Normal light photo of same specimen.

to keep the carbonate chemistry constant, normal air (ambient $PCO_2 = 380$ ppm) pre-saturated with water vapour, was bubbled through the culture media (Table 1). Salinity and pH levels were measured every second day (WTW conductivity meter 330i with TetraCon 325 electrode for salinity; WTW pH 3000 with Schott BlueLine Electrodes calibrated with NIST buffers for pH). To minimize the impact of bacterial growth, changes in salinity due to evaporation, and/or changes in carbonate chemistry, culture media were replaced every 2 weeks. To assess any possible offset over this limited time period, samples were taken at the end of every 2 weeks incubations for analyses of dissolved inorganic carbon (DIC), alkalinity, and seawater elemental composition (measured by ICP-OES) (Tables 1 and 2). DIC samples were micro filtered (0.2 μm) and stored in 13-mL borosilicate flasks free of air-bubbles at 4 °C until they were measured photometrically with an autoanalyzer (Technicon TRAACS 800 Bran + Lübbe, Norderstedt, Germany) with an average precision of 10 μmol kg^{-1} based on triplicate analyses. Samples for alkalinity analyses were stored in 300-mL borosilicate flasks at 4 °C and measured in triplicate by potentiometric titration, resulting in an average precision of 8 μEq kg^{-1} (Brewer et al., 1986). Total alkalinity was calculated from linear Gran Plots (Gran, 1952). Mg and Sr partitioning coefficients, $D_{Me} = (Me/Ca)ca/(Me/Ca)sw$, which represent the distribution of the metal (Me: i.e. Sr and Mg), between calcite (ca) and the culture medium (sw), were calculated for each set of experimental conditions. After one and a half months the experiment was terminated. The culture experiments were carried out at the Alfred Wegener Institute for Polar and Marine Research (Bremerhaven/Germany).

2.2. Measurements with LA-ICP-MS

2.2.1. Cleaning procedures

Since the foraminifera were cultured without sediment, the rigorous cleaning procedure required for specimens

Table 1
Carbonate chemistry of the culture media. The experiments ran for one and a half months. The growth media were changed every 2 weeks. T_0 represents average values of alkalinity and DIC for each new medium. T_{end} represents average values of alkalinity and DIC for each used media. Salinity and pH were measured every second day. Values of Ω were calculated using the Visual Minteq program.

Salinity		T_0 (10 °C)	T_{end} (10 °C)	T_0 (15 °C)	T_{end} (15 °C)	Ω	
						10 °C	15 °C
20	Total alkalinity (μEq kg^{-1})	1480(±12)	1579(±77)	1480(±12)	1588(±62)	0.9	1.0
	DIC (μmol kg^{-1})	1416(±59)	1562(109)	1416(±59)	1558(±16)		
	pH (NBS)	7.96(±0.07)		8.00(±0.06)			
	Average salinity	20.4(±0.2)		20.5(±0.2)			
20 + Ca^{2+}	Total alkalinity (μEq kg^{-1})	1457(±10)	1561(±46)	1457(±10)	1532(±37)	1.4	1.6
	DIC (μmol kg^{-1})	1392(±23)	1504(109)	1392(±23)	1501(±68)		
	pH (NBS)	7.94(±0.07)		7.99(±0.07)			
	Average salinity	20.7(±0.2)		20.5(±0.2)			
33	Total alkalinity (μEq kg^{-1})	2421(±40)	2509(±67)	2421(±40)	2533(±81)	2.4	2.8
	DIC (μmol kg^{-1})	2238(±23)	2362(±95)	2238(±23)	2360(±95)		
	pH (NBS)	8.08(±0.07)		8.11(±0.07)			
	Average salinity	33.0(±0.2)		33.0(±0.2)			
40	Total alkalinity (μEq kg^{-1})	3007(±31)	3131(±100)	3007(±31)	3192(±71)	3.7	4.3
	DIC (μmol kg^{-1})	2718(±127)	2840(±27)	2718(±127)	2844(±128)		
	pH (NBS)	8.14(±0.04)		8.17(±0.06)			
	Average salinity	40.7(±0.2)		40.7(±0.2)			

Table 2
Measured Mg/Ca and Sr/Ca of the growth media in mol/mol. The experiment ran for one and a half months. Growth media were changed every 2 weeks. T_0 represents an average value for each new medium. T_{end} represents an average value of samples taken from each of the used media. Uncertainties (standard deviation (one sigma) calculated per experimental condition) are presented in between brackets.

Target salinity	Mg/Ca		Mg/Ca	
	T_0 (10 °C)	T_{end} (10 °C)	T_0 (15 °C)	T_{end} (15 °C)
20	5.28(±0.07)	5.22	5.28(±0.07)	5.27(±0.01)
20 + Ca	3.09(±0.07)	3.06(±0.03)	3.09(±0.07)	3.07(±0.02)
33	5.29	5.36(±0.01)	5.29	5.32(±0.06)
40	5.47(±0.01)	5.49(±0.01)	5.47(±0.01)	
	Sr/Ca		Sr/Ca	
20	$8.55 \times 10^{-3}(\pm 0.11 \times 10^{-3})$	8.47×10^{-3}	$8.55 \times 10^{-3}(\pm 0.11 \times 10^{-3})$	$8.49 \times 10^{-3}(\pm 0.01 \times 10^{-3})$
20 + Ca	$5.04 \times 10^{-3}(\pm 0.06 \times 10^{-3})$	$5.03 \times 10^{-3}(\pm 0.01 \times 10^{-3})$	$5.04 \times 10^{-3}(\pm 0.06 \times 10^{-3})$	$5.04 \times 10^{-3}(\pm 0.05 \times 10^{-3})$
33	8.35×10^{-3}	$8.45 \times 10^{-3}(\pm 0.02 \times 10^{-3})$	8.35×10^{-3}	$8.45 \times 10^{-3}(\pm 0.02 \times 10^{-3})$
40	$8.56 \times 10^{-3}(\pm 0.03 \times 10^{-3})$	$8.43 \times 10^{-3}(\pm 0.03 \times 10^{-3})$	$8.56 \times 10^{-3}(\pm 0.03 \times 10^{-3})$	

collected from sediment cores (e.g. Barker et al., 2003), was not necessary. Instead, a modified cleaning procedure was adopted in which organic matter is removed by soaking specimens for 30 min in a 3–7% NaOCl solution before analysis (Gaffey and Bronnimann, 1993). A stereomicroscope was used during the cleaning procedure to check optically for contamination and possible damage to the foraminiferal tests. Specimens were removed from the cleaning solution directly after complete bleaching in order to avoid dissolution of the final (often thinner) chambers. After cleaning, samples were thoroughly rinsed with deionised water to ensure complete removal of reagent. Dried foraminifera were fixed on a double-sided adhesive tape and mounted on plastic stubs.

2.2.2. Analytical procedures

The final chamber (F) of each specimen that had formed at least two new chambers in culture was measured at the Department of Earth Sciences—Petrology of the University of Utrecht (The Netherlands), using an Excimer laser (Lambda Physik) with GeoLas 200Q optics inside a helium atmosphere flushed ablation chamber (Reichart et al., 2003) (Fig. 2). Pulse repetition rate was set at 6 Hz, with an energy density at the sample surface of 4 J/cm^2 and ablation craters set at 80 μm in diameter. The ablated material was carried on a He flow, which was diluted with an Ar–He mixture before being analyzed with respect to time (and hence depth) on a quadrupole ICP-MS instrument (Micromass Platform ICP-MS). Analyses were calibrated against National Institute of Standards and Technology SRM 610 glass, using concentration data of Pearce et al. (1997) with Ca as an internal standard. Calcium as an internal standard is ideal, because its concentration is constant at 40 wt% in all foraminiferal tests, and because it allows

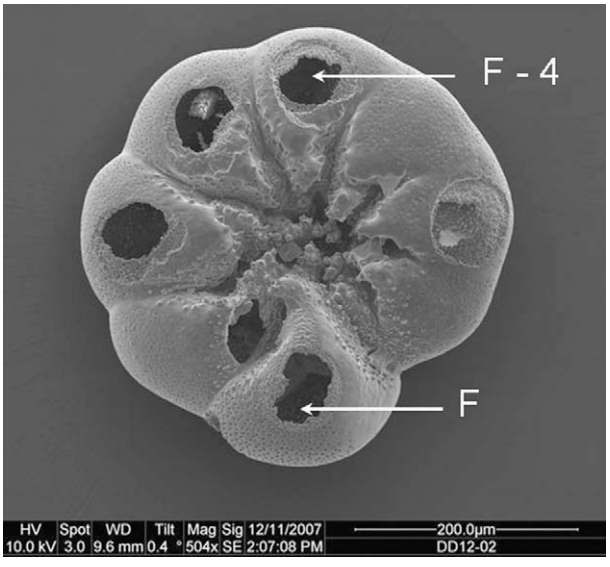

Fig. 2. Scanning electron microscope image of laser ablation craters in *Ammonia Tepida* (F = final chamber). Scale bar is indicated in the lower right corner. In this study, only the analytical results of the final (F) chamber were considered.

direct comparisons with trace metals to Ca ratios from wet-chemical studies. A collision and reaction cell was used to minimize spectral interferences on the minor isotopes of Ca (Mason and Kraan, 2002). ^{44}Ca was used as an internal standard, monitoring ^{42}Ca and ^{43}Ca to check for consistency. The offset between the three isotopes was always less than 2%. Concentrations of Mg and Sr were calculated using ^{24}Mg, ^{26}Mg, and ^{88}Sr. An in house (matrix matched) carbonate standard was used to check for a possible offset due to a different ablation rate on glass and carbonate. No systematic offset was observed. ^{27}Al and ^{55}Mn were monitored to make sure that no contamination was present in part of the profiles used for calculating concentrations. Additional dwell time between isotopes of relative high concentrations and those at much lower levels were added to the analytical setup to avoid the impact of tailing of the more abundant isotopes. Relative precision for Mg, Sr, and Mn, based on analyzing the matrix matched standard before and after each series of 10 measurements, was better than 6.5%.

2.2.3. Signal integration

Element concentrations are calculated for the individual ablation profiles integrating the different isotopes (glitter software). Based on the ^{27}Al counts (parts of the) profiles showing contamination were discarded. Although this approach is somewhat subjective, all profiles were checked for the effect of changing the integrated interval, which was lower than the relative precision in all cases. Because foraminifera were grown in culture vessels without sediment, high count rates of Al isotopes would indicate contamination. Since single laser pulses remove only a few nanometers of material, high resolution trace elements profiles are acquired. Fig. 3 represents time resolved LA-ICP-MS Mg/Ca, Mn/Ca, and Al/Ca ratios measured on two different chambers from a single specimen of *A. tepida*. The profiles obtained by ablating the final chamber (F) (Fig. 2), grown at a temperature of 10 °C and a salinity of 33 psu, and of an older chamber (F-4) grown in the field at unknown conditions, are presented in Fig. 3. For the F chamber, the Mg/Ca count ratio is constant across the chamber wall when excluding the elevated Al counts at the outer surface of the profile indicating a general surface contamination probably generated during manipulation of the specimens. This part of the profile was removed from the calculation of the element ratios. Low Mn/Ca values and the absence of Al within this test wall are likely the result of the calcite being precipitated under clean laboratory conditions. Although the Mg/Ca profile of the F-4 chamber appears to be relatively constant, the higher (and variable) concentration of Mn is characteristics of a dysoxic environment (Reichart et al., 2003), that is common below the surface of tidal flat sediments. The numerous peaks of Al present across the profile of the F-4 chamber grown in natural environment indicate clay on the outside of the test wall and possibly in the pores. This contrasting pattern allows distinguishing between chambers added in the natural environment and those added under controlled culture conditions.

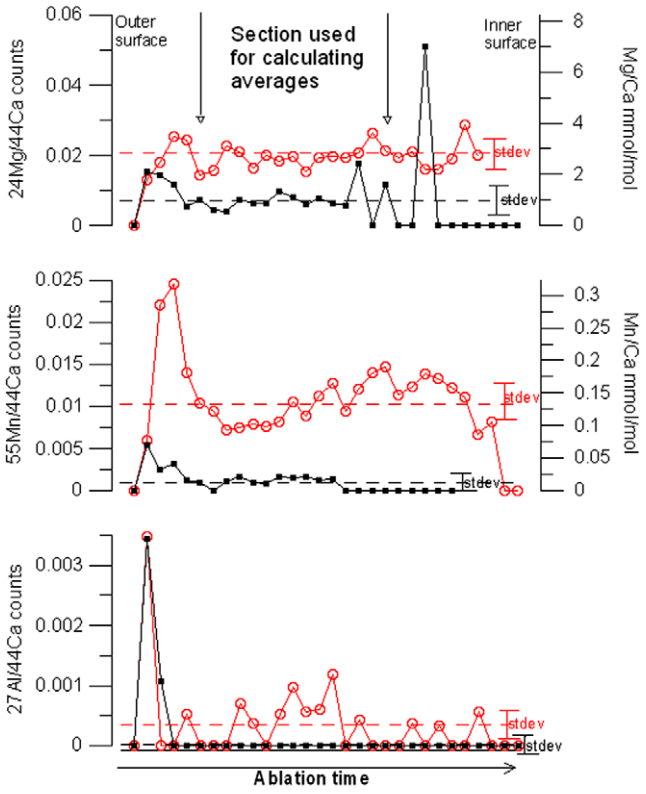

Fig. 3. Time resolved LA-ICP-MS Mg/Ca, Mn/Ca, and Al/Ca ratios of a cleaned *Ammonia tepida*, ablated perpendicular to the chamber-wall surfaces. The empty dots represent the result of the ablation performed on the F-4 chamber grown in natural environment; the small dots represent the results of the ablation on the final (F) chamber grown under laboratory conditions (salinity 33, temperature 10 °C). Standard deviations of the average value are given as error bars. Horizontal dashed lines illustrate mean ratios averaged for the entire profile of each plot. The profiles were ablated from the outside (left) towards the inside (right).

2.3. Carbonate system

Evaporation and dilution of sea water alter the concentrations of Mg, Sr, and Ca. Since they would be enriched or depleted proportionally, the ratios of these elements (Mg/Ca and Sr/Ca) remain constant. However, total ion concentration is affected as well as the carbonate chemistry. For example an increase in salinity from 33 to 40 psu increases both $[Ca^{2+}]$ and $[CO_3^{2-}]$, and the alkalinity by approximately 20%, resulting in an increase of the calcite saturation state (or Ω where $\Omega =$ Ion Activity Product (IAP)/Ksp with Ksp representing the solubility product of calcite). Because both $[Ca^{2+}]$ and $[CO_3^{2-}]$ determine the IAP, changes in salinity alter Ω quadratically. In addition, Ω was altered independently of salinity in the salinity 20 + Ca experiment. The extra added $[Ca^{2+}]$ increased Ω from 0.9 to 1.4 and from 1 to 1.6 at 10 and 15 °C, respectively. The carbonate system was calculated from alkalinity, DIC, temperature, and salinity using the chemical speciation program Visual Minteq (Gustafsson, 2004) (Table 1). As can be seen from Table 1, DIC and Alkalinity increased over the course of the experiments (due to evaporation). For that reason the mean values of the concentrations measured at the start and end of the experiments were used to calculate Ω.

3. RESULTS

3.1. New calcite and survival rates

Almost all specimens survived the experiment despite altered salinity. None of the chambers added during the incubations show abnormalities. The number of new chambers added, however, varies as a function of salinity. The number of specimens that grew new chambers (recognized by fluorescence (Fig. 1)) is greater than 50% across all experiments. For specimens grown at a salinity of 20 psu (conditions close to the salinity in their natural habitat, 24 psu) and grown at a salinity of 20 + Ca, more than 85% grew new chambers (Table 3). At identical salinities the number of chambers added per specimen is higher at 15 °C than at 10 °C. Detailed results of the LA-ICP-MS measurements are presented in Table 4. To exclude possible effects of ontogeny, analyses were restricted to the final (F) chamber of specimens from a size range between 350 μm and 500 μm. The limited size of individual chambers (<100 μm), did not allow multiple ablation craters on a single test chamber. Therefore, only one measurement was performed per specimen (always on the final (F) chamber). The number of specimens analyzed per experimental condition is presented in Tables 3 and 4.

Table 3
Number of individuals *of Ammonia tepida* at the beginning of the experiments, number of specimens that formed new calcite, total number of newly formed chambers, and number of LA-ICP-MS measurements used for elemental concentrations.

	Experiment target salinity	Number of specimens at the beginning of the experiment	Number of specimens that formed new chambers	Total of new chambers added per experimental conditions	Total of LA-ICP-MS measurements performed on F chambers per experimental conditions
10 °C	20	30	28	49	16
	20 + Ca	30	27	44	11
	33	30	18	32	9
	40	30	22	33	12
15 °C	20	30	27	55	21
	20 + Ca	30	26	52	15
	33	30	23	44	17
	40	30	25	39	18

3.2. Elemental concentrations

3.2.1. Experiment salinity 20, 33, and 40 psu

The average Mg/Ca ratio of *A. tepida* is overall relatively low (between 0.5 and 1.3 mmol/mol; Table 4 and Fig. 4a) when compared to other foraminiferal species (e.g. Anand and Elderfield, 2005; Bentov and Erez, 2006). The value of the Sr/Ca ratios varies between 0.8 and 1.6 mmol/mol which is comparable to other foraminiferal species (on average 0.9–1.6 mmol/mol; Lea, 1999) (Table 4 and Fig. 4b). Partition coefficients for Mg and Sr were calculated for each experiment (Table 4) and plotted versus salinity (Fig. 4c and d). D_{Mg} increases with increasing temperature (Fig. 4c). To deconvolve changes in D related directly to salinity or indirectly through associated changes in Ω (see Section 2.3), D_{Mg} and D_{Sr} were plotted versus Ω (Fig. 4e and f). Clearly both D_{Mg} and D_{Sr} of the foraminiferal calcite are positively correlated with the calcite saturation state of the culture medium.

3.2.2. Experiment salinity 20 + Ca

After addition of Ca to the growth medium, Mg/Ca and Sr/Ca ratios of seawater varied from 5.3 to 3.1 mol/mol, and from 8.6×10^{-3} to 5.0×10^{-3} mol/mol, respectively. The addition of Ca to the growth medium results in a decreased Sr/Ca ratio measured in the test wall (Table 4 and Fig. 4b). The Sr/Ca ratio of the test is proportional to the Sr/Ca ratio of the growth media, also the partitioning coefficient for Sr is nearly identical in the salinity 20 + Ca experiment when compared to the normal salinity 20 psu experiment (1.53×10^{-1} and 1.46×10^{-1} at 10 °C, and 1.52×10^{-1} and 1.49×10^{-1} at 15 °C, with and without Ca, respectively) (Table 4 and Fig. 4d). On the contrary, the Mg/Ca ratios of the specimens grown in the salinity 20 + Ca experiment are only slightly lower than the values of the specimens grown in the salinity 20 psu experiment without additional Ca. The additional Ca and the associated increase in Ω results in an significant increase of the Mg partition coefficient (Table 4 and Fig. 4c).

4. DISCUSSION

4.1. Mg/Ca response to temperature

For inorganically precipitated calcite it is known that the D_{Mg} increases with increasing temperature (e.g. Chilingar, 1962; Katz, 1973). One of the best inorganic data sets (Oomori et al., 1987) fits well to an exponential function with a rate constant of 3.1 ± 0.4% per °C between 10 and 50 °C. In foraminifera the increase of Mg within the test can be up to 3 times stronger (9 ± 1% per °C; Nurnberg, 1995; Nurnberg et al., 1996; Rosenthal et al., 1997; Lea et al., 1999; Lea, 2003). Temperature is, therefore, assumed to impact physiological processes regulating the incorporation of Mg in foraminiferal calcite (Rosenthal et al., 1997). The D_{Mg} of *A. tepida* increases with 4.1%, 4.6%, and 5.5% per °C (temperature range 10–15 °C) for salinities of 20, 33, and 40 psu, respectively (increase of the Mg/Ca ratio by 4.2%, 4.5%, and 5.5% per °C for salinities of 20, 33, and 40 psu, respectively). Toyofuku et al. (2000) report on the calibration of two neritic high-Mg benthic species, *Planoglabratella opercularis* and *Quinqueloculina yabei* (Asano), in culture experiments and show that the D_{Mg} in these species increases by 1.8% and 2.6% per °C, respectively, which is much smaller than observed for low-Mg foraminifera. This led to the hypothesis that the Mg/Ca response to temperature might scale with the magnesium content of calcite (Lea, 2003). However, the moderate response of the low-Mg species *A. tepida* (0.6–1.3 mmol/mol at 10–15 °C) (Fig. 4a), is not in line with this hypothesis. Although physiological processes may still be responsible for foraminiferal interspecific differences, the mechanism by which temperature influences the incorporation of Mg in foraminiferal calcite remains a subject of debate (for an overview, see Bentov and Erez, 2006).

4.2. Sr/Ca response to temperature

Compared to the impact of temperature on the Mg incorporation, the Sr incorporation increase in foraminiferal calcite from 10 to 15 °C is relatively small (Fig. 4d).

Table 4
Detailed results of LA-ICP-MS measurements per experimental conditions. Only a unique measurement performed on the F chamber is reported per specimen. Mg/Ca and Sr/Ca are presented in mmol/mol. D_{Mg} and D_{Sr} were calculated following $D_{Me} = (Me/Ca)ca/(Me/Ca)sw$. Mean values are presented with uncertainties (standard deviation (one sigma) calculated per experimental conditions).

Specimen	Mg/Ca (mmol/mol)	D_{Mg}	Sr/Ca (mmol/mol)	D_{Sr}	Specimen	Mg/Ca (mmol/mol)	D_{Mg}	Sr/Ca (mmol/mol)	D_{Sr}
20‰ 10 °C					*20‰ 15 °C*				
1	0.41	7.82×10^{-5}	1.20	1.42×10^{-1}	1	0.89	1.68×10^{-4}	1.35	1.59×10^{-1}
2	0.39	7.44×10^{-5}	1.18	1.38×10^{-1}	2	0.86	1.63×10^{-4}	1.21	1.42×10^{-1}
3	0.37	6.96×10^{-5}	0.96	1.13×10^{-1}	3	0.75	1.42×10^{-4}	1.34	1.58×10^{-1}
4	0.87	1.65×10^{-4}	1.35	1.59×10^{-1}	4	1.02	1.93×10^{-4}	1.38	1.62×10^{-1}
5	0.53	1.00×10^{-4}	1.29	1.52×10^{-1}	5	0.83	1.58×10^{-4}	1.16	1.37×10^{-1}
6	0.81	1.55×10^{-4}	1.17	1.38×10^{-1}	6	0.60	1.14×10^{-4}	1.19	1.40×10^{-1}
7	0.33	6.32×10^{-5}	1.39	1.63×10^{-1}	7	0.91	1.72×10^{-4}	1.05	1.23×10^{-1}
8	0.48	9.20×10^{-5}	1.16	1.36×10^{-1}	8	0.83	1.57×10^{-4}	1.22	1.43×10^{-1}
9	0.85	1.62×10^{-4}	1.02	1.20×10^{-1}	9	0.66	1.26×10^{-4}	1.23	1.44×10^{-1}
10	0.75	1.43×10^{-4}	1.30	1.52×10^{-1}	10	0.52	9.86×10^{-5}	1.24	1.46×10^{-1}
11	0.49	9.30×10^{-5}	1.43	1.69×10^{-1}	11	0.59	1.12×10^{-4}	1.02	1.19×10^{-1}
12	0.76	1.44×10^{-4}	1.30	1.53×10^{-1}	12	0.57	1.07×10^{-4}	1.27	1.49×10^{-1}
13	1.04	1.99×10^{-4}	1.22	1.43×10^{-1}	13	0.68	1.29×10^{-4}	1.29	1.51×10^{-1}
14	0.81	1.55×10^{-4}	1.38	1.62×10^{-1}	14	0.67	1.27×10^{-4}	1.30	1.52×10^{-1}
15	0.66	1.27×10^{-4}	1.20	1.42×10^{-1}	15	0.70	1.33×10^{-4}	1.29	1.51×10^{-1}
16	0.73	1.40×10^{-4}	1.24	1.46×10^{-1}	16	0.79	1.50×10^{-4}	1.14	1.33×10^{-1}
Mean	0.64 ± 0.22	$1.23 \times 10^{-4} \pm 0.42 \times 10^{-4}$	1.24 ± 0.13	$1.46 \times 10^{-1} \pm 0.15 \times 10^{-1}$	17	0.69	1.31×10^{-4}	1.26	1.48×10^{-1}
					18	0.95	1.79×10^{-4}	1.37	1.61×10^{-1}
					19	0.98	1.87×10^{-4}	1.49	1.74×10^{-1}
					20	0.88	1.67×10^{-4}	1.53	1.79×10^{-1}
					21	1.00	1.89×10^{-4}	1.30	1.53×10^{-1}
					Mean	0.78 ± 0.15	$1.48 \times 10^{-4} \pm 0.28 \times 10^{-4}$	1.27 ± 0.12	$1.49 \times 10^{-1} \pm 0.14 \times 10^{-1}$
20‰ + Ca 10 °C					*20‰ + Ca 15 °C*				
1	0.47	1.53×10^{-4}	0.83	1.65×10^{-1}	1	0.41	1.32×10^{-4}	0.72	1.42×10^{-1}
2	0.57	1.86×10^{-4}	0.76	1.52×10^{-1}	2	1.57	1.84×10^{-4}	0.71	1.41×10^{-1}
3	0.60	1.94×10^{-4}	0.87	1.74×10^{-1}	3	0.74	2.40×10^{-4}	0.73	1.44×10^{-1}
4	0.36	1.17×10^{-4}	0.78	1.55×10^{-1}	4	0.52	1.69×10^{-4}	0.87	1.73×10^{-1}
5	0.46	1.48×10^{-4}	0.73	1.45×10^{-1}	5	0.37	1.20×10^{-4}	0.87	1.73×10^{-1}
6	0.51	1.66×10^{-4}	0.81	1.31×10^{-1}	6	0.70	2.28×10^{-4}	0.80	1.59×10^{-1}
7	0.41	1.32×10^{-4}	0.68	1.35×10^{-1}	7	0.84	2.72×10^{-4}	0.77	1.53×10^{-1}
8	0.56	1.83×10^{-4}	0.69	1.36×10^{-1}	8	0.57	1.85×10^{-4}	0.82	1.62×10^{-1}
9	0.41	1.33×10^{-4}	0.77	1.53×10^{-1}	9	0.61	1.99×10^{-4}	0.77	1.54×10^{-1}
10	0.60	1.96×10^{-4}	0.83	1.66×10^{-1}	10	0.88	2.85×10^{-4}	0.84	1.66×10^{-1}
11	0.54	1.75×10^{-4}	0.74	1.47×10^{-1}	11	0.60	1.96×10^{-4}	0.81	1.60×10^{-1}
Mean	0.50 ± 0.08	$1.62 \times 10^{-4} \pm 0.26 \times 10^{-4}$	0.77 ± 0.06	$1.53 \times 10^{-1} \pm 0.12 \times 10^{-1}$	12	0.74	2.39×10^{-4}	0.66	1.30×10^{-1}

33‰ Ca 10 °C				
1	0.59	1.10×10^{-4}	1.42	1.69×10^{-1}
2	0.92	1.72×10^{-4}	1.27	1.51×10^{-1}
3	1.07	2.00×10^{-4}	1.31	1.56×10^{-1}
4	1.33	2.49×10^{-4}	1.22	1.45×10^{-1}
5	0.65	1.22×10^{-4}	1.23	1.46×10^{-1}
6	0.67	1.26×10^{-4}	1.69	2.02×10^{-1}
7	1.17	2.19×10^{-4}	1.34	1.60×10^{-1}
8	1.00	1.87×10^{-4}	1.54	1.84×10^{-1}
9	0.53	9.89×10^{-5}	1.33	1.59×10^{-1}
Mean	0.88 ± 0.28	$1.65 \times 10^{-4} \pm 0.53 \times 10^{-4}$	1.37 ± 0.16	$1.63 \times 10^{-1} \pm 0.19 \times 10^{-1}$
40‰ Ca 10 °C				
1	1.23	2.25×10^{-4}	1.53	1.80×10^{-1}
2	1.41	2.57×10^{-4}	1.49	1.75×10^{-1}
3	0.88	1.60×10^{-4}	1.42	1.67×10^{-1}
4	1.17	2.14×10^{-4}	1.43	1.68×10^{-1}
5	1.33	2.43×10^{-4}	1.40	1.65×10^{-1}
6	1.24	2.26×10^{-4}	1.30	1.53×10^{-1}
7	1.00	1.83×10^{-4}	1.18	1.39×10^{-1}
8	0.93	1.69×10^{-4}	1.52	1.79×10^{-1}
9	0.88	1.61×10^{-4}	1.55	1.83×10^{-1}
10	0.82	1.50×10^{-4}	1.37	1.83×10^{-1}
11	0.83	1.51×10^{-4}	1.59	1.87×10^{-1}
12	0.89	1.62×10^{-4}	1.35	1.59×10^{-1}
Mean	1.05 ± 0.21	$1.92 \times 10^{-4} \pm 0.38 \times 10^{-4}$	1.43 ± 0.12	$1.68 \times 10^{-1} \pm .014 \times 10^{-1}$
13	0.75	2.44×10^{-4}	0.77	1.52×10^{-1}
14	0.64	2.10×10^{-4}	0.68	1.34×10^{-1}
15	0.59	1.91×10^{-4}	0.66	1.31×10^{-1}
Mean	0.64 ± 0.14	$2.08 \times 10^{-4} \pm 0.46 \times 10^{-4}$	0.76 ± 0.07	$1.52 \times 10^{-1} \pm 0.14 \times 10^{-1}$
33‰ Ca 15 °C				
1	0.91	1.71×10^{-4}	1.49	1.77×10^{-1}
2	0.77	1.44×10^{-4}	1.64	1.95×10^{-1}
3	1.01	1.90×10^{-4}	1.32	1.57×10^{-1}
4	1.02	1.92×10^{-4}	1.36	1.61×10^{-1}
5	1.47	2.77×10^{-4}	1.55	1.84×10^{-1}
6	1.22	2.29×10^{-4}	1.15	1.36×10^{-1}
7	1.77	1.45×10^{-4}	1.37	1.63×10^{-1}
8	1.31	2.47×10^{-4}	1.52	1.80×10^{-1}
9	0.71	1.34×10^{-4}	1.38	1.64×10^{-1}
10	0.86	1.62×10^{-4}	1.68	1.99×10^{-1}
11	0.72	1.35×10^{-4}	1.72	2.05×10^{-1}
12	0.79	1.48×10^{-4}	1.49	1.77×10^{-1}
13	1.55	2.92×10^{-4}	1.16	1.37×10^{-1}
14	1.74	3.28×10^{-4}	1.33	1.58×10^{-1}
15	1.04	1.95×10^{-4}	1.19	1.41×10^{-1}
16	1.30	2.46×10^{-4}	1.53	1.82×10^{-1}
17	1.16	2.17×10^{-4}	1.44	1.72×10^{-1}
Mean	1.08 ± 0.31	$2.03 \times 10^{-4} \pm 0.58 \times 10^{-4}$	1.43 ± 0.17	$1.69 \times 10^{-1} \pm 0.20 \times 10^{-1}$
40‰ Ca 15 °C				
1	0.82	1.49×10^{-4}	1.38	1.62×10^{-1}
2	1.44	2.64×10^{-4}	1.66	1.93×10^{-1}
3	1.40	2.56×10^{-4}	1.75	2.04×10^{-1}
4	0.83	1.51×10^{-4}	1.78	2.08×10^{-1}
5	0.86	1.57×10^{-4}	1.59	1.86×10^{-1}
6	1.56	2.85×10^{-4}	1.40	1.63×10^{-1}
7	1.60	2.93×10^{-4}	1.79	2.09×10^{-1}
8	1.46	2.68×10^{-4}	1.53	1.79×10^{-1}
9	0.98	1.79×10^{-4}	1.43	1.67×10^{-1}
10	1.52	2.78×10^{-4}	2.15	2.52×10^{-1}
11	1.36	2.49×10^{-4}	1.75	2.04×10^{-1}
12	1.27	2.33×10^{-4}	1.54	1.80×10^{-1}
13	1.96	3.58×10^{-4}	1.34	1.56×10^{-1}
14	1.44	2.62×10^{-4}	1.59	1.86×10^{-1}
15	1.66	3.03×10^{-4}	1.45	1.70×10^{-1}
16	0.99	1.81×10^{-4}	1.65	1.93×10^{-1}
17	2.17	3.96×10^{-4}	1.64	1.82×10^{-1}
18	0.88	1.61×10^{-4}	1.43	1.67×10^{-1}
Mean	1.34 ± 0.39	$2.45 \times 10^{-4} \pm 0.71 \times 10^{-4}$	1.60 ± 0.20	$1.87 \times 10^{-1} \pm 0.23 \times 10^{-1}$

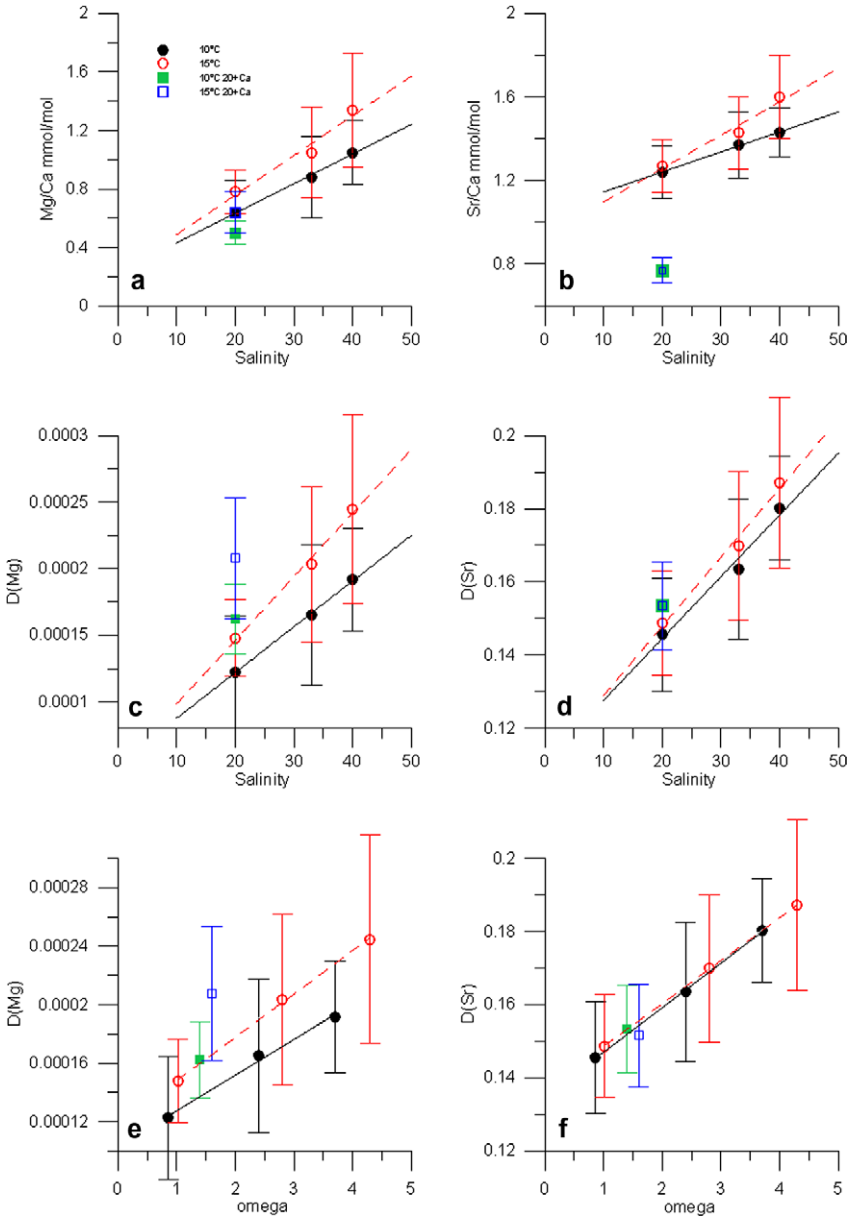

Fig. 4. Mg/Ca ratio (a), Sr/Ca ratio (b), Mg partitioning coefficient (D_{Mg}) (c), and Sr partitioning coefficient (D_{Sr}) (d) in *Ammonia tepida* test versus salinity. Mg Partitioning coefficient (D_{Mg}) (e) and Sr partitioning coefficient (D_{Sr}) (f) in *A. tepida* test versus $CaCO_3$ saturation state (Ω) calculated with Visual Minteq program. Every point is the average of specimens grown under similar experimental conditions (10 °C, line and closed circles; 15 °C, dashed line and open circles). The results obtained in the experiment salinity 20 + Ca are plotted on the same graphs (10 °C, closed squares; 15 °C, open squares).

Previous studies have shown that Sr/Ca ratios increase by 0.4–1% per °C in the planktonic species *Orbulina universa* and *Globigerina bulloides* (Lea et al., 1999; Russell et al., 2004) suggesting that temperature only accounts for a small part of the observed Sr/Ca variation in foraminiferal calcite. While Rosenthal et al. (1997) did not observe any Sr-temperature dependency in deep benthic foraminifera, Rathburn and DeDeckker (1997) and Reichart et al. (2003) report a significant temperature correlation for the Sr/Ca ratio (6% increase per °C between −2 and 9 °C in *C. wuellerstorfi*, and 7% increase per °C between 2 and 13 °C in *Hoeglundina elegans*, respectively). Even if the Sr/Ca ratio in the tests of benthic foraminifera has been shown to decrease with increasing water depth (McCorkle et al., 1995; Elderfield et al., 1996; Rathburn and DeDeckker, 1997; Rosenthal et al., 1997) the effect of temperature is hard to deconvolve from other parameters such as salinity, pressure (Lea et al., 1999), and seawater $[CO_3^{2-}]$ (Rathmann and Kuhnert, 2008). We show that *A. tepida* D_{Sr} increases with 0.4%, 0.6%, and 2.2% per °C (temperature range 10–15 °C), for salinities of 20, 33, and 40 psu, respectively (increase of the Sr/Ca ratio by 0.5%, 0.8%,

and 2.5% per °C, for salinities 20, 33, and 40 psu). The different slopes for the different salinities suggest that the observed increase is not only related to temperature, but apparently also depend on the calcite saturation state (Ω) which covaries with salinity. Moreover, increasing temperature also affects the Ion Activity Product (IAP) as temperature changes Ksp and thereby Ω. When plotting D_{Sr} versus Ω (Fig. 4f), the temperature effect disappears. Temperature seems to influence the incorporation of Sr only through its impact on Ω. Compared to inorganic precipitated calcite (Lorens, 1981; Tesoriero and Pankow, 1996) the Sr/Ca ratio in foraminiferal calcite is significantly higher and on average 0.9–1.6 mmol/mol (Lea, 1999; 1.2–1.6 mmol/mol for *A. tepida*). In contrast to Mg, growth rate effects determined from inorganic precipitation can explain alone the temperature effect on Sr incorporation. Additional culture experiments are required to verify whether this assumption can be extended to other benthic species from deeper parts of the water column.

4.3. Mg/Ca response to salinity

At both temperatures, the amount of Mg incorporated increases with increasing salinity. We demonstrate that, when all others parameters are kept constant, linear percentage increase in D_{Mg} per psu are 2.8 at 10 °C, and 3.3 at 15 °C, for the salinity intervals 20–40 psu. In terms of D_{Mg}, a salinity increase of 2 psu is equivalent to a 1 °C temperature increase (see Section 4.1) (For the salinity intervals 20–40 psu, the Mg/Ca ratio increases linearly with 3.2% and 3.6% per psu, for 10 and 15 °C, respectively). These results are similar to those observed by Lea et al. (1999) (increase of Mg/Ca ratio by $4 \pm 3\%$ per psu, salinity range 27–39 psu) and Kisakurek et al. (2008) (increase of Mg/C a ratio by $5 \pm 3\%$ per psu, salinity range 32–41 psu) on planktonic species (*O. universa* and *Globigerinoides ruber*, respectively). On the contrary, these results differ from the observation by Nurnberg et al. (1996) who report 7–10% Mg/Ca ratio increase per salinity unit for the *Globigerinoides sacculifer* species, (salinity range 26–44). However, these calculations were based on only two specimens and should therefore be considered carefully. To our knowledge there is no previous culture study relating the impact of salinity to the Mg incorporation in benthic foraminifera.

4.3.1. Impact of vacuolization on foraminiferal Mg/Ca

Calcite precipitation by perforate foraminifera is under strong biological control, starting with the uptake of seawater and subsequent modification and storage of the ions necessary for $CaCO_3$ precipitation (Erez, 2003; Bentov and Erez, 2005, 2006). The low-Mg/Ca ratios in *A. tepida* for example, can only be explained by a physiological discrimination between the Mg^{2+} and Ca^{2+} ions in vacuolized seawater. Controlling the composition of the parent solution from which the calcite precipitates, allows controlling polymorph and mineral phase composition. Modification of the composition within the vacuoles is thought to take place during transport to the calcification site and/or at the calcification site ("privileged space") itself. For a detailed description on the various physiological processes, see Bentov and Erez (2006). If we assume that higher salinity vacuolized seawater contains elevated concentrations of all ions (e.g. Ca^{2+} and Mg^{2+}) and that: (1) the vacuole content is modified during transport to the calcification site, (2) the number of pumps or channels regulating the Mg^{2+} flux is genetically controlled and therefore independent of the seawater composition, and (3) the vacuole migration time to be constant at constant temperature, then, a higher concentration of Mg should arrive at the calcification site. Active vacuolization would therefore explain the higher D_{Mg} observed at higher salinity (and higher Ω), and vice versa.

4.4. Sr/Ca response to salinity

A significant increase of the D_{Sr} with increasing salinity is observed in our experiments (Fig. 4d). Lea et al. (1999) report that Sr/Ca ratios of *O. universa* grown at salinities 27, 33, and 39 psu, and a constant temperature (22 °C), increase with $0.8 \pm 0.3\%$ per salinity unit. This is in good agreement with our data where the D_{Sr} increases linearly by 0.8% and 1.3% for the salinity intervals 20–40 psu, at 10 °C and 15 °C, respectively (Sr/Ca ratio increases linearly by 0.8% and 1.3% for the salinity intervals 20–40 psu, at 10 °C and 15 °C, respectively). The observed D_{Sr} of *A. tepida* is significantly higher than those obtained from inorganic precipitation experiments, indicating that Sr is subjected to biological regulations. As discussed for Mg, vacuolization of high salinity seawater gives rise to a higher concentration of Sr in the vacuoles. Vice versa, lower salinity would result in a lower D_{Sr} of the foraminiferal calcite. To explain the higher concentration of Sr present in the foraminiferal calcite as compared to inorganic precipitation, a process increasing the Sr/Ca ratio in the vacuoles has to be involved in parallel to one decreasing the Mg/Ca ratio. Sr selective transport is rather unlikely considering that such a mechanism is unknown in biological pathways (Langer et al., 2006). Ca depletion would also cause an increase of the Mg/Ca ratio, and therefore, would be possible only if an even stronger depletion of Mg occurred at the same site.

A positive correlation between D_{Sr} and growth rate is well documented for inorganically precipitated calcite (Lorens, 1981; Tesoriero and Pankow, 1996; Nehrke et al., 2007). Similarly, our results demonstrate that an increase in D_{Sr} is also positively correlated to an increase in Ω (Fig. 4f). Although a straightforward comparison between inorganic precipitation and organic calcification is difficult, an increase of the calcification rate could explain the increase of Sr incorporation. Since chamber formation is not a continuous process over the course of the experiment it is not possible to translate test weight or wall thickness into absolute calcification rates. Moreover, the precipitation rate of inorganic calcite is not linearly correlated with the calcite saturation state of the parent solution (Nielsen, 1964). However, based on the observation that the $pH/[CO_3^{2-}]$ in the vacuoles increase on their way to the site of calcification (de Nooijer et al., 2009), we assume that the calcite saturation state increase significantly above that of the bulk medium. Therefore the increase in Sr incorporation in the calcite of *A. tepida* with increasing salinity,

and hence with increasing Ω, could be due to an increase of the calcification rate.

4.5. Deconvolution of salinity and calcite saturation state

Fig. 4c shows that the addition of Ca to the growth media induced an increase of D_{Mg} at both temperatures (10 °C and 15 °C). Addition of Ca decreases the Mg/Ca ratio of the growth media. Vacuolized seawater (see Section 4.3) in this experimental condition is enriched in calcium and therefore results in a lower Mg/Ca ratio in the vacuoles. If during the transport of the vacuoles to the site of calcification and/or at the site of calcification itself, Mg is selectively removed at a constant rate, as assumed above, a lower Mg/Ca ratio is expected at the site of calcification and hence in the foraminiferal calcite. However, Fig. 4a shows that the Mg/Ca ratio measured in foraminiferal calcite is only slightly lower than the average ratio found in calcite in the experiment with a salinity of 20 psu without additional Ca. Although surface seawater in the ocean is about 5 times supersaturated with respect to calcite, inorganic precipitation of calcium carbonate does not occur since the presence of Mg^{2+} and phosphates inhibit nucleation and crystal growth of $CaCO_3$ in seawater (Morse and Mackenzie, 1990). When considering the calcification process in foraminifera growing in media enriched in Ca, the relative concentration of Mg is depleted. Magnesium is supposed to be removed during transport of the vacuoles to the site of calcification and/or at the site of calcification itself, until the Mg concentration is low enough to allow calcium carbonate to precipitate. Since the initial seawater is already depleted in Mg, the ionic concentration of the vacuoles will reach threshold Mg values earlier. This implies that the depletion of Mg is limited, possibly in order to allow the foraminifera to maintain control over the calcification process (crystals deposition and organization) (Debenay et al., 2000; Erez, 2003). Such a mechanism could explain the similarity in the Mg/Ca ratio measured in the calcite grown at salinity 20 psu and salinity 20 + Ca, and the significant increase of the D_{Mg} observed for the salinity 20 + Ca experiment. These results seem to reveal an inhibitory effect of Mg on biogenic calcite precipitation. This is in good agreement with the results from Segev and Erez (2006), who observed a gradual and consistent decrease in calcification of the two species *Amphistegina lobifera*, and *Am. lessonii* for specimens cultured in growth media with Mg/Ca ratios higher than 1. With regard to Sr, the addition of Ca results in a significant decrease of the Sr/Ca values. However, the D_{Sr} shows only a small increase when compared to the results obtained for the salinity 20 psu experiment (Fig. 4d), variations which can be explained by changes in Ω (see Section 2.3).

4.6. Comparison of Mg and Sr behaviour

In our experiments, Mg and Sr incorporation into the test of *A. tepida* have been observed to respond differently. Three differences were found: (1) for identical experimental conditions D_{Mg} is lower while D_{Sr} is higher compared to the partition coefficients in inorganic precipitation. (2) Although the incorporation of Mg and Sr are both increasing with increasing temperature, the impact of temperature is stronger for Mg than for Sr. The impact of temperature on Sr incorporation disappears when corrected for Ω, while this is not the case for Mg. (3) The addition of Ca in the salinity 20 + Ca experiment induces a significant increase in $D_{Mg,}$ but has no significant impact on the D_{Sr}. These observations seem to indicate that Mg and Sr are incorporated into foraminiferal calcite via different pathways.

5. SUMMARY/CONCLUSION

The calcitic tests of *A. tepida* have low-Mg concentrations compared to most other species. Magnesium incorporation increases with increasing temperature (D_{Mg} increases by 4.1%, 4.6%, and 5.5% per °C (temperature range 10–15 °C for salinities of 20, 33, and 40 psu, respectively), but to a lesser extent than previously described for other low-Mg calcite foraminifera. This does not support the hypothesis that the foraminiferal Mg/Ca response to temperature might scale with the magnesium content of calcite (Lea, 2003). In contrast to Mg, the impact of temperature on the Sr incorporation is relatively small (D_{Sr} increases by 0.4%, 0.6%, and 2.2% per °C (temperature range 10–15 °C for salinities of 20, 33, and 40 psu, respectively). The different slopes for the different salinities suggest that the observed increase in Sr is not only related to temperature, but apparently also depend on the calcite saturation state (Ω) which covaries with salinity. The increase of the Sr incorporation with increasing temperature can be explained by the associated increase of the calcite saturation state. Hence, calcite saturation state might control the response of the Sr incorporation to changes in temperature.

At both temperatures (10 and 15 °C), the amount of Mg incorporated increases linearly with increasing salinity (increase of D_{Mg} by 2.8% (10 °C), and 3.3% (15 °C) per psu, for the 20–40 psu salinity intervals). In terms of paleo-reconstructions based on the Mg partitioning coefficient of *A. tepida*, a salinity increase of 2 psu is equivalent to a 1 °C temperature increase. Increased Mg incorporation with increasing salinity may be explained by the following process: a higher concentration of Mg^{2+} is taken up into vacuoles at higher salinity leading to higher concentration of Mg arriving at the site of calcification and thus being incorporated.

Similarly as observed for Mg, a significant increase of the D_{Sr} with increasing salinity is observed in our experiments (D_{Sr} increases linearly by 0.8% and 1.3% for the salinity intervals 20–40 psu, at 10 °C and 15 °C, respectively). In terms of paleo-reconstructions based on the Sr partitioning coefficient of *A. tepida*, a salinity increase of 1 psu is equivalent to a 1 °C temperature increase. Two possible processes can be put forward: (1) as described for Mg, a higher concentration of Sr^{2+} is taken up at higher salinity leading to higher concentration in Sr arriving at the site of calcification and being incorporated and (2) the Sr incorporation increases at higher salinity due to an increase of "calcification rate".

The addition of Ca to the growth media induced an increase of D_{Mg} at both temperatures (10 °C and 15 °C). This

increase, which cannot be explained by changes in the calcite saturation state, seems to be due to an inhibitory effect of Mg on biogenic calcite precipitation. In contrast, the small increase of the D_{Sr} observed after addition of Ca^{2+} to the growth media, can be explained by changes in the calcite saturation state. The Sr incorporation into the tests of *A. tepida* is directly dependent on the Sr/Ca ratio of the growth media.

ACKNOWLEDGMENTS

This work was supported by the German Research Foundation (DFG) under Grant No. BI 432/4-2 ("PaleoSalt"), and by the European Science Foundation (ESF) under the EUROCORES Programme EuroCLIMATE through Contract No. ERAS-CT-2003-980409 of the European Commission, DG Research, FP6. We would like to thank two anonymous reviewers for improving the manuscript significantly and Lennart de Nooijer for helpful comments on an earlier version of the manuscript. We thank Gijs Nobbe and Paul Mason for technical support with LA-ICP-MS, Beate Mueller (formally Hollmann) for assistance with the culture experiments, and Anja Terbruggen for DIC analysis.

REFERENCES

Anand P., Elderfield H. and Conte M. H. (2003) Calibration of Mg/Ca thermometry in planktonic foraminifera from a sediment trap time series. *Paleoceanography* **18**.

Anand P. and Elderfield H. (2005) Variability of Mg/Ca and Sr/Ca between and within the planktonic foraminifers *Globigerina bulloides* and *Globorotalia truncatulinoides*. *Geochem. Geophys. Geosyst.* **6**.

Barker S., Greaves M. and Elderfield H. (2003) A study of cleaning procedures used for foraminiferal Mg/Ca paleothermometry. *Geochem. Geophys. Geosyst.* **4**.

Barker S., Cacho I., Benway H. and Tachikawa K. (2005) Planktonic foraminiferal Mg/Ca as a proxy for past oceanic temperatures: a methodological overview and data compilation for the last glacial maximum. *Quatern. Sci. Rev.* **24**, 821–834.

Bentov S. and Erez J. (2005) Novel observations on biomineralization processes in foraminifera and implications for Mg/Ca ratio in the shells. *Geology* **33**, 841–844.

Bentov S. and Erez J. (2006) Impact of biomineralization processes on the Mg content of foraminiferal shells: a biological perspective. *Geochem. Geophys. Geosyst.* **7**.

Bernhard J. M., Blanks J. K., Hintz C. J. and Chandler G. T. (2004) Use of the fluorescent calcite marker calcein to label foraminiferal tests. *J. Foramin. Res.* **34**, 96–101.

Brewer P. G., Bradshow A. L. and Williams R. T. (1986) Measurement of total carbon dioxide and alkalinity in the North Atlantic Ocean in 1981. In *The Changing Carbon Cycle—A Global Analysis* (eds. J. R. Trabalka and D. E. Reichle). Springer-Verlag, New York.

Broecker W. S. and Peng T.-H. (1982) *Tracers in the Sea*. Lamont Doherty Geological Observatory, Palisades, NY.

Chilingar G. V. (1962) Dependence on temperature of Ca/Mg ratio of skeletal structures of organisms and direct chemical precipitates out of sea water. *Bull. South. Calif.: Acad. Sci.* **61**, 45–61.

de Nooijer L. J., Toyofuku T. and Kitazato H. (2009) Foraminifera promote calcification by elevating their intracellular pH. *Proc. Natl Acad. Sci. USA* **106**, 15374–15378.

Debenay J. P., Guillou J. J., Geslin E. and Lesourd M. (2000) Crystallization of calcite in foraminiferal tests. *Micropaleontology* **46**, 87–94.

Dissard D., Nehrke G., Reichart G.-J., Nouet J. and Bijma J. (2009) Effect of the fluorescent indicator calcein on Mg and Sr incorporation into foraminiferal calcite. *Geochem. Geophy. Geosyst.* **10**.

Elderfield H., Bertram C. J. and Erez J. (1996) Biomineralization model for the incorporation of trace elements into foraminiferal calcium carbonate. *Earth Planet. Sci. Lett.* **142**, 409–423.

Elderfield H., Vautravers M. and Cooper M. (2002) The relationship between shell size and Mg/Ca, Sr/Ca, delta O-18, and delta C-13 of species of planktonic foraminifera. *Geochem. Geophys. Geosyst.* **3**.

Elderfield H., Yu J., Anand P., Kiefer T. and Nyland B. (2006) Calibrations for benthic foraminiferal Mg/Ca paleothermometry and the carbonate ion hypothesis. *Earth Planet. Sci. Lett.* **250**, 633–649.

Erez J. (2003) The source of ions for biomineralization in foraminifera and their implications for paleoceanographic proxies. *Rev. Mineral. Geochem.* **54**, 115–149.

Ferguson J. E., Henderson G. M., Kucera M. and Rickaby R. E. M. (2008) Systematic change of foraminiferal Mg/Ca ratios across a strong salinity gradient. *Earth Planet. Sci. Lett.* **265**, 153–166.

Gaffey S. J. and Bronnimann C. E. (1993) Effects of bleaching on organic and mineral phases in biogenic carbonates. *J. Sed. Petrol.* **63**, 752–754.

Gran G. (1952) Determination of the equivalence point in potentiometric titrations of seawater with hydrochloric acid. *Oceanol. Acta* **5**, 209–218.

Groeneveld J., Nurnberg D., Tiedemann R., Reichart G. J., Steph S., Reuning L., Crudeli D. and Mason P. (2008) Foraminiferal Mg/Ca increase in the Caribbean during the pliocene: Western Atlantic Warm Pool formation, salinity influence, or diagenetic overprint? *Geochem. Geophys. Geosyst.* **9**.

Gustafsson J. P. (2004) Visual Minteq Version 2.53.KTH, Stockholm, Sweden. Available from: <http://www.lwr.kth.se/English/OurSoftware/vminteq/index.htm/>).

Hastings D. W., Russell A. D. and Emerson S. R. (1998) Foraminiferal magnesium in *Globeriginoides sacculifer* as a paleotemperature proxy. *Paleoceanography* **13**, 161–169.

Hayward B. W., Holzmann M., Grenfell H. R., Pawlowski J. and Triggs C. M. (2004) Morphological distinction of molecular types in *Ammonia*—towards a taxonomic revision of the world's most commonly misidentified foraminifera. *Mar. Micropaleontol.* **50**, 237–271.

Hintz C. J., Shaw T. J., Bernhard J. M., Chandler G. T., McCorkle D. C. and Blanks J. K. (2006) Trace/minor element: calcium ratios in cultured benthic foraminifera: Part II. Ontogenetic variation. *Geochim. Cosmochim. Acta* **70**, 1964–1976.

Honisch B. and Hemming N. G. (2004) Ground-truthing the boron isotope-paleo-pH proxy in planktonic foraminifera shells: partial dissolution and shell size effects. *Paleoceanography* **19**.

Katz A. (1973) The interaction of magnesium with calcite during crystal growth at 25–90 °C and one atmosphere. *Geochim. Cosmochim. Acta* **37**, 1563–1586.

Kisakurek B., Eisenhauer A., Bohm F., Garbe-Schonberg D. and Erez J. (2008) Controls on shell Mg/Ca and Sr/Ca in cultured planktonic foraminiferan, *Globigerinoides ruber* (white). *Earth Planet. Sci. Lett.* **273**, 260–269.

Langer G., Geisen M., Baumann K. H., Klas J., Riebesell U., Thoms S. and Young J. R. (2006) Species-specific responses of calcifying algae to changing seawater carbonate chemistry. *Geochem. Geophys. Geosyst.* **7**.

Lea D. W. (1999) Trace elements in foraminiferal calcite. In *Modern Foraminifera* (ed. B. K. S. Gupta). Kluwer Academic Publishers.

Lea D. W., Mashiotta T. A. and Spero H. J. (1999) Controls on magnesium and strontium uptake in planktonic foraminifera determined by live culturing. *Geochim. Cosmochim. Acta* **63**, 2369–2379.

Lea D. W. (2003) Elemental and isotope proxies of past ocean temperatures. In *The Oceans and Marine Geochemistry* (ed. H. Elderfield). Elsevier, Amsterdam.

Lear C. H., Rosenthal Y. and Slowey N. (2002) Benthic foraminiferal Mg/Ca-paleothermometry: a revised core-top calibration. *Geochim. Cosmochim. Acta* **66**, 3375–3387.

Lorens R. B. (1981) Sr, Cd, Mn and Co distribution coefficients in calcite as a function of calcite precipitation rate. *Geochim. Cosmochim. Acta* **45**, 553–561.

Mason P. R. D. and Kraan W. J. (2002) Attenuation of spectral interferences during laser ablation inductively coupled plasma mass spectrometry (LA-ICP-MS) using an rf only collision and reaction. *J. Anal. At. Spectrom.* **17**, 858–867.

McCorkle D. C., Martin P. A., Lea D. W. and Klinkhammer G. P. (1995) Evidence of a dissolution effect on benthic foraminiferal shell chemistry—Delta-C-13, Cd/Ca, Ba/Ca, and Sr/Ca results from the Ontong Java Plateau. *Paleoceanography* **10**, 699–714.

Morse J. W. and Mackenzie F. T. (1990) *Geochemistry of Sedimentary Carbonates*. Elsevier, New York.

Nehrke G., Reichart G. J., Van Cappellen P., Meile C. and Bijma J. (2007) Dependence of calcite growth rate and Sr partitioning on solution stoichiometry: non-Kossel crystal growth. *Geochim. Cosmochim. Acta* **71**, 2240–2249.

Nielsen A. E. (1964) *Kinetics of Precipitation*. Pergamon Press, New York.

Nurnberg D. (1995) Magnesium in test of *Neogloboquadrina pachyderma* sinistral from high northern and southern latitudes. *J. Foramin. Res.* **25**, 350–368.

Nurnberg D., Bijma J. and Hemleben C. (1996) Assessing the reliability of magnesium in foraminiferal calcite as a proxy for water mass temperatures. *Geochim. Cosmochim. Acta* **60**, 803–814.

Oomori T., Kaneshima H. and Maezato Y. (1987) Distribution coefficient of Mg^{2+} ions between calcite and solution at 10–50 °C. *Mar. Chem.* **20**, 327–336.

Pearce N. J. G., Perkins W. T., Westgate J. A., Gorton M. P., Jackson S. E., Neal C. R. and Chenery S. P. (1997) A compilation of new and published major and trace element data for NIST SRM 610 and NIST SRM 612 glass reference materials. *Geostand. Newsl.: J. Geostand. Geoanal.* **21**, 115–144.

Rathburn A. E. and DeDeckker P. (1997) Magnesium and strontium compositions of recent benthic foraminifera from the Coral Sea, Australia and Prydz Bay, Antarctica. *Mar. Micropaleontol.* **32**, 231–248.

Rathmann S. and Kuhnert H. (2008) Carbonate ion effect on Mg/Ca, Sr/Ca and stable isotopes on the benthic foraminifera *Oridorsalis umbonatus* off Namibia. *Mar. Micropaleontol.* **66**, 120–133.

Reichart G. J., Jorissen F., Anschutz P. and Mason P. R. D. (2003) Single foraminiferal test chemistry records the marine environment. *Geology* **31**, 355–358.

Rink S., Kuhl M., Bijma J. and Spero H. J. (1998) Microsensor studies of photosynthesis and respiration in the symbiotic foraminifer *Orbulina universa*. *Mar. Biol.* **131**, 583–595.

Rosenthal Y., Boyle E. A. and Slowey N. (1997) Temperature control on the incorporation of magnesium, strontium, fluorine, and cadmium into benthic foraminiferal shells from Little Bahama Bank: prospects for thermocline paleoceanography. *Geochim. Cosmochim. Acta* **61**, 3633–3643.

Rosenthal Y., Lear C. H., Oppo D. W. and Linsley B. K. (2006) Temperature and carbonate ion effects on Mg/Ca and Sr/Ca ratios in benthic foraminifera: aragonitic species *Hoeglundina elegans*. *Paleoceanography* **21**.

Russell A. D., Honisch B., Spero H. J. and Lea D. W. (2004) Effects of seawater carbonate ion concentration and temperature on shell U, Mg, and Sr in cultured planktonic foraminifera. *Geochim. Cosmochim. Acta* **68**, 4347–4361.

Sadekov A., Eggins S. M., DeDeckker P. and Kroon D. (2008) Uncertainties in seawater thermometry deriving from intratest and intertest Mg/Ca variability in *Globigerinoides ruber*. *Paleoceanography* **23**.

Segev E. and Erez J. (2006) Effect of Mg/Ca ratio in seawater on shell composition in shallow benthic foraminifera. *Geochem. Geophys. Geosyst.* **7**.

Tesoriero A. J. and Pankow J. F. (1996) Solid solution partitioning of Sr^{2+}, Ba^{2+}, and Cd^{2+} to calcite. *Geochim. Cosmochim. Acta* **60**, 1053–1063.

Toyofuku T., Kitazato H., Kawahata H., Tsuchiya M. and Nohara M. (2000) Evaluation of Mg/Ca thermometry in foraminifera: comparison of experimental results and measurements in nature. *Paleoceanography* **15**, 456–464.

Associate editor: Anders Meibom